

Special Lagrangian torus fibrations of complete intersection Calabi–Yau manifolds: a geometric conjecture

To Shing-Tung Yau on his 65th birthday

David R. Morrison* and M. Ronen Plesser†

* Departments of Mathematics and Physics, U.C. Santa Barbara, Santa Barbara CA 93106

† Center for Geometry and Theoretical Physics, Duke University, Durham NC 27708

Abstract

For complete intersection Calabi–Yau manifolds in toric varieties, Gross and Haase–Zharkov have given a conjectural combinatorial description of the special Lagrangian torus fibrations whose existence was predicted by Strominger, Yau and Zaslow. We present a geometric version of this construction, generalizing an earlier conjecture of the first author.

Federer observed in his classic monograph [9] that a compact complex submanifold of a Kähler manifold minimizes volume in its homology class, due to a local property of the Kähler form which follows from the Wirtinger inequality. Harvey and Lawson [24] generalized this to the notion of *calibrated submanifold* in 1982, and found several other classes of submanifolds with a homological volume-minimizing property, including the *special Lagrangian submanifolds of a Ricci-flat Kähler manifold*. Thanks to Yau’s proof [45, 46] of the Calabi conjecture [5], we have a rich supply of such Ricci-flat manifolds.

A Calabi–Yau manifold Z has both a Ricci-flat Kähler form ω_Z and a non-vanishing holomorphic form of top degree Ω_Z ; the special Lagrangian condition on a submanifold $L \subset Z$ (whose real dimension is half that of Z) simply says that both ω_Z and $\text{Re}(\Omega_Z)$ vanish when restricted to L . In spite of the simplicity of the definition, the structure of special Lagrangian submanifolds is still largely unknown. However, given a special Lagrangian submanifold L in a fixed Calabi–Yau manifold Z , the local deformation theory [30] and global deformation theory [25] of L within Z are known, and in particular it is known that the deformation space is a real manifold of dimension $b_1(L)$. Thus, if Z has complex dimension n and L has the topology of a real n -torus T^n and if moreover the nearby deformations of L are disjoint from L , then the resulting family of tori will determine a fibration of an open subset of Z .

Nearly twenty years ago, Strominger, Yau, and Zaslow [44] conjectured a relationship between the phenomenon of mirror symmetry which had been discovered in the physics community [1, 6, 11] and fibrations of Calabi–Yau manifolds by special Lagrangian tori (with singular

fibers allowed). According to the conjecture, special Lagrangian torus fibrations should exist for Calabi–Yau manifolds which have mirror partners, and the special Lagrangian torus fibrations on a mirror pair of Calabi–Yau manifolds should be dual to each other fiber by fiber (at least once certain corrections to the geometry have been made which are associated to holomorphic disks whose boundary lies on a special Lagrangian torus). The original physics argument is expected to apply when the moduli of the Calabi–Yau metric are near the boundary of the moduli space. More precisely, the complex structure should be near a degeneration with “maximally unipotent monodromy” [32, 8, 31] and the Kähler class should be deep within the Kähler cone. By restricting attention to small neighborhoods of the boundary, and focussing on properties of the base of the fibration, Gross and Siebert were led to a beautiful reformulation of the conjecture as a problem in algebraic geometry [17], and much progress has been made on that reformulation [18–20].¹

1 Geometric conjectures

Returning to the original version of the problem, even almost twenty years later we still lack the analytic tools to directly analyze special Lagrangian submanifolds of a compact Calabi–Yau manifold. However, building on some local analysis of Joyce [26–29] as well as early work on the problem by Zharkov [47], Gross [12–14] and Ruan [35–43], the first author formulated in [34] a series of conjectures about the structure of these fibrations. Following [34], we only state the conjectures for Calabi–Yau threefolds.

The first conjecture, essentially due to Gross [12–14] and Ruan [35–37], concerns the combinatorial properties of the fibration.

Conjecture 1. *Let $\pi : Z \rightarrow B$ be a special Lagrangian T^3 fibration of a compact Calabi–Yau threefold with respect to a Calabi–Yau metric whose compatible complex structure is sufficiently close to a boundary point with maximally unipotent monodromy, and whose Kähler class is sufficiently deep in the Kähler cone. Then*

i) The discriminant locus of the fibration retracts onto a trivalent graph D , which we call the combinatorial discriminant locus.

ii) For any loop around an edge of D , the monodromy on either $H^1 \cong H_2$ or H_1 of the 3-tori is conjugate to

$$M = \begin{pmatrix} 1 & 0 & 1 \\ 0 & 1 & 0 \\ 0 & 0 & 1 \end{pmatrix}. \tag{1.1}$$

In particular, both monodromy actions have a 2-dimensional fixed plane.

iii) The vertices of D come in two types: near a positive vertex, the three monodromy actions on $H^1 \cong H_2$ near the vertex have fixed planes whose intersection is 1-dimensional, while the three monodromy actions on H_1 have a common 2-dimensional fixed plane.

¹For a recent review, see [16].

In an appropriate basis, the monodromy matrices on H_1 take the form

$$\begin{pmatrix} 1 & 0 & 1 \\ 0 & 1 & 0 \\ 0 & 0 & 1 \end{pmatrix}, \quad \begin{pmatrix} 1 & 0 & 0 \\ 0 & 1 & 1 \\ 0 & 0 & 1 \end{pmatrix}, \quad \begin{pmatrix} 1 & 0 & -1 \\ 0 & 1 & -1 \\ 0 & 0 & 1 \end{pmatrix}. \quad (1.2)$$

On the other hand, near a negative vertex, the three monodromy actions on $H^1 \cong H_2$ near the vertex have a common 2-dimensional fixed plane, while the three monodromy actions on H_1 have fixed planes whose intersection is 1-dimensional. In an appropriate basis, the monodromy matrices on H_1 take the form

$$\begin{pmatrix} 1 & 0 & 1 \\ 0 & 1 & 0 \\ 0 & 0 & 1 \end{pmatrix}, \quad \begin{pmatrix} 1 & 1 & 0 \\ 0 & 1 & 0 \\ 0 & 0 & 1 \end{pmatrix}, \quad \begin{pmatrix} 1 & -1 & -1 \\ 0 & 1 & 0 \\ 0 & 0 & 1 \end{pmatrix}. \quad (1.3)$$

- iv) There are open neighborhoods $U_P \subset B$ of the vertices P of D such that each fiber of π over a point not in $\bigcup_P U_P$ has Euler characteristic 0, and such that the Euler characteristic of $\pi^{-1}(U_P)$ is either 1 or -1 , depending on whether P is a positive or negative vertex.

The second conjecture, formulated in [34], is more geometric in nature. It should be stressed that there is very little evidence for this geometric conjecture at the present moment. However, it appears to be geometrically very natural, and assuming its truth has helped to clarify a number of the tricky combinatorial issues associated with mirror symmetry.

Conjecture 2. *Let $\pi : Z \rightarrow B$ be a special Lagrangian T^3 fibration of a compact Calabi–Yau threefold with respect to a Calabi–Yau metric whose compatible complex structure is sufficiently close to a boundary point with maximally unipotent monodromy, and whose Kähler class is sufficiently deep in the Kähler cone. Then*

- i) *The set $C \subset Z$ of singular points of fibers of π is a complex subvariety of Z of complex dimension 1.*
- ii) *All singular points of C are transverse triple points, locally of the form $\{z_1 z_2 = z_1 z_3 = z_2 z_3 = 0\}$ for local complex coordinates z_1, z_2, z_3 .*
- iii) *For each connected component C_α of C , the image $\pi(C_\alpha)$ has the topology of a disc with $g(C_\alpha)$ holes, and the map $\pi|_{C_\alpha}$ is generically 2-to-1 onto its image. The image $\pi(C_\alpha)$ has a distinguished boundary component which contains the images of all points in $\text{Sing}(C) \cap C_\alpha$.*
- iv) *There is a graph $D_\alpha \subset \pi(C_\alpha)$ to which $\pi(C_\alpha)$ retracts. D_α has univalent vertices on the boundary of $\pi(C_\alpha)$ at the images of all points in $\text{Sing}(C) \cap C_\alpha$, and has only trivalent vertices in the interior. The graph $D = \bigcup_\alpha D_\alpha$ is the combinatorial discriminant locus of Conjecture 1.*
- v) *The map π puts the singular points of C in one-to-one correspondence with the positive vertices of D , which are located at the intersections of the various D_α . The negative vertices of D are the interior vertices of the various D_α 's.*

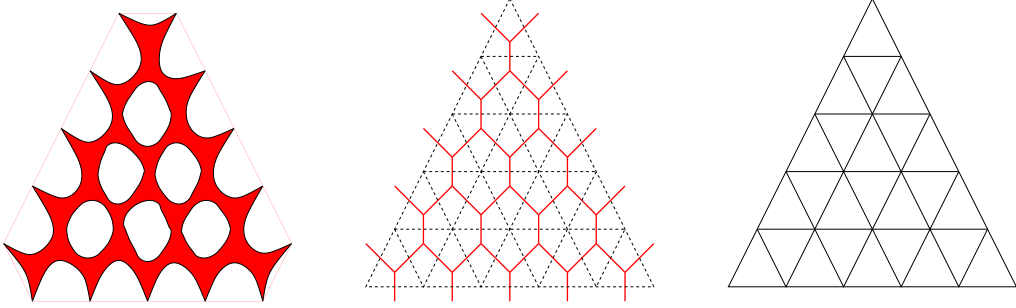


Figure 1: Ingredients of the geometric conjecture for the quintic threefold: the image of C_{ij} under the moment map, a graph to which it retracts, and a part of the corresponding triangulation of the dual polytope for $\mathbb{C}\mathbb{P}_{ij}^2$.

The singular locus C , its image $\pi(C)$ and the graph D were conjecturally described for Calabi–Yau hypersurfaces in toric varieties in [34], motivated by a construction of Zharkov [47]. We illustrate the conjecture in the case of quintic hypersurfaces in $\mathbb{C}\mathbb{P}^4$. Let x_1, \dots, x_5 be the homogeneous coordinates of $\mathbb{C}\mathbb{P}^4$, and let $F(x_1, \dots, x_5)$ be the defining equation of the hypersurface. The components of C are the quintic plane curves

$$C_{ij} := \{x_i = x_j = F = 0\} \subset \mathbb{C}\mathbb{P}_{ij}^2.$$

They meet along the sets

$$P_{ijk} := \{x_i = x_j = x_k = F = 0\},$$

each of which consists of five points. The image $\pi(C_{ij})$ is isomorphic to the image of C_{ij} under the *moment map* $\mu_{ij} : \mathbb{C}\mathbb{P}_{ij}^2 \rightarrow \mathbb{R}^2$, as illustrated on the left side of Figure 1. The graph D_{ij} , illustrated in the middle of Figure 1, is a tropical limit of C_{ij} to which $\mu_{ij}(C_{ij})$ retracts; it is determined by a triangulation of the dual polytope of $\mathbb{C}\mathbb{P}_{ij}^2$ (illustrated on the right side of Figure 1).

The goal of this paper is to describe C , $\pi(C)$, and D for complete intersections in toric varieties.

2 Nef partitions and singular limits

The combinatorial tool needed to describe a Calabi–Yau complete intersection in a toric variety is a “nef partition,” first defined by Borisov [4] and later expanded upon by Batyrev and Borisov [2, 3]. Let $X = X_T$ be a compact toric variety of dimension d determined by² a triangulation T of a polytope $\nabla^\vee \subset N_{\mathbb{R}} \cong \mathbb{R}^d$. (The fan determining X_T consists of cones over simplices in T ; alternatively, the vertices of T provide a construction of X_T as a geometric quotient: see [10, 7]).

²The polytope determining X is often denoted by Δ in the literature. For the current construction, although we will indeed encounter a polytope $\Delta \subset N_{\mathbb{R}}$, it is distinct from ∇^\vee except in the hypersurface case.

A vertex e_a of T determines a toric divisor H_a . A family of complete intersections Z is determined by a *nef partition* of ∇^\vee with r parts. This is a partition of the vertices e_1, \dots, e_N into r disjoint groups

$$\{e_1, \dots, e_N\} = \coprod_{i=1}^r E^{(i)}, \quad \text{where } E^{(i)} = \{e_{i,1}, \dots, e_{i,d(i)}\}, \quad (2.1)$$

with the property that the associated line bundles

$$\mathcal{L}_i := \mathcal{O}_X \left(\sum_{\alpha=1}^{d_i} H_{i,\alpha} \right)$$

are all nef.³

We then have

$$\nabla^\vee = \text{Conv} \left(\Delta^{(1)} \cup \dots \cup \Delta^{(r)} \right), \quad (2.2)$$

where

$$\Delta^{(i)} = \text{Conv} \left(\{0\} \cup E^{(i)} \right). \quad (2.3)$$

Note that the product of the nef line bundles

$$\otimes_i \mathcal{L}_i = \mathcal{O}_X (H_1 + \dots + H_N) = \mathcal{O}_X (-K_X)$$

is also nef, which implies that ∇^\vee is a relexive polyhedron.

Our Calabi–Yau n -fold is given as the complete intersection

$$Z = \{F_1 = \dots = F_r = 0\} \subset X,$$

where F_i is a homogeneous polynomial of the same degree as $\prod_{\alpha=1}^{d(i)} x_{i,\alpha}$, i.e., it is a global section of the line bundle \mathcal{L}_i .

We restrict attention here to the case of an *irreducible* nef partition. A partition is irreducible if there is no subset $\{i_1, \dots, i_k\} \subset \{1, \dots, r\}$ such that $\Delta^{(i_1)} + \dots + \Delta^{(i_k)}$ contains 0 in its interior. Up to a possible refinement of the lattice any nef partition is a direct sum of irreducibles [23]. The Calabi–Yau spaces associated to reducible partitions are thus discrete quotients of products of complete intersections of lower dimension.

For any $\vec{\alpha} = (\alpha_1, \dots, \alpha_r)$ with $1 \leq \alpha_i \leq d(i)$, we define

$$X_{\vec{\alpha}} = \bigcap_{i=1}^r H_{i,\alpha_i}.$$

Note that each $X_{\vec{\alpha}}$ is a (possibly empty) toric subvariety of X of codimension r .

For each $X_{\vec{\alpha}}$ and each toric divisor $H_{\ell,m}$ with $m \neq \alpha_\ell$, the intersection $X_{\vec{\alpha}} \cap H_{\ell,m}$ coincides with $X_{\vec{\alpha}} \cap X_{\vec{\beta}}$ where $\vec{\beta}$ is obtained from $\vec{\alpha}$ by

$$\beta_i = \begin{cases} \alpha_i & \text{if } i \neq \ell \\ m & \text{if } i = \ell \end{cases}.$$

³This condition can be expressed combinatorially [4].

It follows that if we remove

$$X_{\vec{\alpha}} \cap \left(\bigcup_{\vec{\beta} \neq \vec{\alpha}} X_{\vec{\beta}} \right)$$

from $X_{\vec{\alpha}}$, the remainder is isomorphic to $(\mathbb{C}^*)^n$, and hence is fibered by real n -tori.

We can form a natural family of Calabi–Yau varieties by taking the i^{th} defining polynomial to be $tF_i + (1 - t) \prod_{\alpha=1}^{d(i)} x_{i,\alpha}$; as $t \rightarrow 0$, this approaches the “large complex structure limit.” By construction, the limiting Calabi–Yau variety in this large complex structure limit is

$$Z_0 := \bigcup_{\vec{\alpha}} X_{\vec{\alpha}}.$$

Points on Z_0 which belong to only one $X_{\vec{\alpha}}$ are part of the torus fibration.

As in the hypersurface case, and as in Zharkov’s early work [47], we expect that the T^n fibration on the large complex structure limit will deform along with the complex structure to nearby Calabi–Yau manifolds.

We can now formulate the main new conjecture of this paper.

Main Conjecture. *If Z is close to the large complex structure limit Z_0 , then the n -torus fibration on Z_0 deforms to a fibration $\pi : Z \rightarrow B$ by real n -tori. When singular fibers are included, the parameter space for the fibration is diffeomorphic to S^n .*

Moreover, the set of singular points of fibers of this T^n -fibration is a complex subvariety of complex codimension two in Z , described as follows. For each part of the nef partition, there is a subvariety $C^{(i)}$ of codimension two and a subvariety of $P^{(i)}$ of codimension three, defined by

$$C^{(i)} = \bigcup_{1 \leq \lambda_1 < \lambda_2 \leq d(i)} Z \cap H_{i,\lambda_1} \cap H_{i,\lambda_2}, \text{ and}$$

$$P^{(i)} = \bigcup_{1 \leq \mu_1 < \mu_2 < \mu_3 \leq d(i)} Z \cap H_{i,\mu_1} \cap H_{i,\mu_2} \cap H_{i,\mu_3}.$$

The conjectured set of singular points of fibers of the T^n fibration is $C := C^{(1)} \cup \dots \cup C^{(r)}$.

Note that for Z generic, the components $C_{\lambda_1, \lambda_2}^{(i)}$ of $C^{(i)}$ are all nonsingular, and also that $P^{(i)}$ is the singular locus of $C^{(i)}$; each component $P_{\mu_1, \mu_2, \mu_3}^{(i)}$ serves as the intersection of three of the components of $C^{(i)}$. Note also that for $i \neq j$, $C^{(i)} \cap C^{(j)}$ has complex codimension at least four in Z .

The singular set C is a complex curve in the case of Calabi–Yau threefolds. We will describe $\pi(C)$ in the next section, and the combinatorial discriminant D to which it retracts in section 4.

One easy consequence of this conjecture is a formula for the Euler characteristic of Z when $n \leq 3$. We explain this in examples.

The case $n = 1$ is not interesting because there is nothing of codimension 2, and the Calabi–Yau 1-fold is always fibered by T^1 ’s over S^1 , with no singular fibers.

In the case $n = 2$, C is a collection of points. Each singular fiber contributes 1 to the Euler characteristic, and the total space is a K3 surface, so we expect precisely 24 points in C . Let us see how that works in various cases.

A complete intersection of degree (d_1, \dots, d_k) in \mathbb{P}^{k+2} (with each $d_k \geq 2$) is a K3 surface if $\sum d_i = k + 3$. We divide the homogeneous coordinates into k groups with d_j elements in the j^{th} group. In the j^{th} group, we should intersect the K3 surface with one of $\binom{d_j}{2}$ pairs of hyperplanes, and each such intersection will have $\prod d_i$ points. Thus, the total number of points is

$$\left(\sum_j \binom{d_j}{2} \right) \prod_i d_i.$$

Remarkably, this turns out to be 24 in every case:

| (d_1, \dots, d_k) | $\sum_j \binom{d_j}{2}$ | $\prod_i d_i$ | # points |
|---------------------|--|-------------------------|----------|
| (4) | $\binom{4}{2} = 6$ | 4 | 24 |
| (3, 2) | $\binom{3}{2} + \binom{2}{2} = 4$ | $3 \cdot 2 = 6$ | 24 |
| (2, 2, 2) | $\binom{2}{2} + \binom{2}{2} + \binom{2}{2} = 3$ | $2 \cdot 2 \cdot 2 = 8$ | 24 |

Now we consider the case $n = 3$. Each $C_{\lambda_1, \lambda_2}^{(i)}$ is a nonsingular complex curve, and they meet three at a time along the sets $P_{\mu_1, \mu_2, \mu_3}^{(i)}$. Note that the various complex curves $C^{(1)}, C^{(2)}, \dots, C^{(r)}$ are pairwise disjoint (since their intersection has codimension 4 on Z).

To compute the Euler characteristic, we remove all of the intersection points from each $C_{\lambda_1, \lambda_2}^{(i)}$, leaving us with a punctured complex curve $\tilde{C}_{\lambda_1, \lambda_2}^{(i)}$ with negative Euler characteristic. This retracts onto a graph consisting solely of negative vertices, with the number of vertices being the absolute value of the Euler characteristic of $\tilde{C}_{\lambda_1, \lambda_2}^{(i)}$. Since the fiber of each positive (resp. negative) vertex contributes Euler characteristic $+1$ (resp. -1) of the Calabi–Yau threefold, the overall Euler characteristic is

$$\sum \#(P_{\mu_1, \mu_2, \mu_3}^{(i)}) - \sum |\chi(\tilde{C}_{\lambda_1, \lambda_2}^{(i)})|.$$

For a complete intersection of degree $(4, 2)$ in \mathbb{P}^6 , we divide the homogeneous coordinates into a group of 4 and a group of 2. There are $\binom{4}{2} = 6$ complex curves from the first group, and $\binom{2}{2} = 1$ from the second group. The complex curves are complete intersections of degree $(4, 2)$ in \mathbb{P}^3 , and have genus $1 + 4 \cdot 2 = 9$ and Euler characteristic $-2 \cdot (4 \cdot 2) = -16$. There are $\binom{4}{3} = 4$ toric subvarieties of codimension three associated to the first group but none from the second group (since $\binom{2}{3} = 0$); each meets the Calabi–Yau in $4 \cdot 2 = 8$ points. In the first group, the complex curves are each punctured along $4 - 2$ toric subvarieties (corresponding to the two remaining coordinates in the first group, out of 4), so at a total of $(4 - 2) \cdot 4 \cdot 2 = 16$ points. Thus, the Euler characteristic of these punctured curves is $-2 \cdot (4 \cdot 2) - (4 - 2) \cdot (4 \cdot 2) = -4 \cdot (4 \cdot 2) = -32$. On the other hand, the Euler characteristic of the (unpunctured) curve in the second group $-2 \cdot (4 \cdot 2) - (2 - 2) \cdot (4 \cdot 2) = -2 \cdot (4 \cdot 2) = -16$, where we are thinking of it being punctured along $2 - 2$ toric subvarieties. The total Euler characteristic is thus

$$\left(\binom{4}{3} + \binom{2}{3} \right) \cdot (4 \cdot 2) - \binom{4}{2} \cdot 4 \cdot (4 \cdot 2) - \binom{2}{2} \cdot 2 \cdot (4 \cdot 2) = -176.$$

The analysis of other complete intersections is similar, and we indicate each one by a parallel equation which indicates how the Euler characteristic is calculated. For the quintic hypersurface, the calculation is

$$\binom{5}{3} \cdot (5) - \binom{5}{2} \cdot 5 \cdot (5) = -200.$$

For the complete intersection of degree (3, 3) in \mathbb{P}^6 , the calculation is

$$\left(\binom{3}{3} + \binom{3}{3} \right) \cdot (3 \cdot 3) - \binom{3}{2} \cdot 3 \cdot (3 \cdot 3) - \binom{3}{2} \cdot 3 \cdot (3 \cdot 3) = -144.$$

For the complete intersection of degree (3, 2, 2) in \mathbb{P}^7 , the calculation is

$$\left(\binom{3}{3} + \binom{2}{3} + \binom{2}{3} \right) \cdot (3 \cdot 2 \cdot 2) - \binom{3}{2} \cdot 3 \cdot (3 \cdot 2 \cdot 2) - \binom{2}{2} \cdot 2 \cdot (3 \cdot 2 \cdot 2) - \binom{2}{2} \cdot 2 \cdot (3 \cdot 2 \cdot 2) = -144.$$

Finally, for the complete intersection of degree (2, 2, 2, 2) in \mathbb{P}^8 , the calculation is

$$\left(4 \times \binom{2}{3} \right) \cdot (2^4) - 4 \times \left(\binom{2}{2} \cdot 2 \cdot (2^4) \right) = -128.$$

Notice that in this last case, the first term is zero: there are no toric subvarieties of codimension three, and no positive vertices, in the calculation.

3 The image under π , and a further limit

We expect each component of $\pi(C)$ to have real codimension one in S^n , with an amoeba-like structure analogous to the one shown in the left side of Figure 1. However, this is not easy to see directly.

To describe our proposal for the structure of $\pi(C)$, we need to consider a further degeneration of the components of the singular locus. (This degeneration will also be useful in section 4 in understanding the structure of the combinatorial discriminant.) Each of the components $C_{\lambda_1, \lambda_2}^{(i)}$ is itself a complete intersection in the toric variety $H_{i, \lambda_1} \cap H_{i, \lambda_2}$, and we will take a further degeneration of this complete intersection. We do this by replacing each F_j , $j \neq i$ by the corresponding homogeneous monomial $\prod_{\alpha=1}^{d(j)} x_{j, \alpha}$.

For any $\vec{\alpha} = (\alpha_1, \dots, \alpha_r)$ with $1 \leq \alpha_i \leq d(i)$, we define

$$Y_{\vec{\alpha}}^{(i)} = \bigcap_{\substack{j=1 \\ j \neq i}}^r H_{j, \alpha_j},$$

and note that each $Y_{\vec{\alpha}}^{(i)}$ is a (possibly empty) toric subvariety of X of codimension $r-1$. Just as in the earlier analysis of Z_0 , it is easy to see that

$$\bigcap_{j \neq i} \left\{ \prod_{\alpha=1}^{d(j)} x_{j, \alpha} = 0 \right\} = \bigcup_{\vec{\alpha}} Y_{\vec{\alpha}}^{(i)}.$$

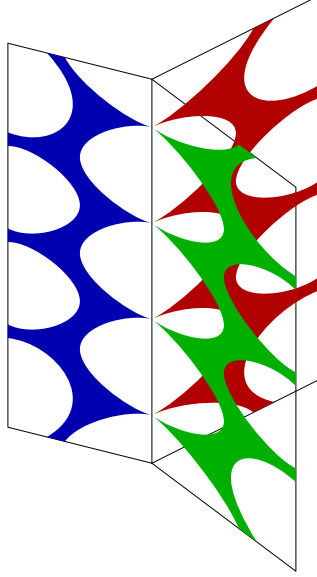


Figure 2: Components of $\pi(C^{(i)})$ meeting three-at-a-time.

Our further degeneration thus replaces $C_{\lambda_1, \lambda_2}^{(i)}$ by

$$\widehat{C}_{\lambda_1, \lambda_2}^{(i)} = \{F_i = 0\} \cap H_{i, \lambda_1} \cap H_{i, \lambda_2} \cap \bigcup_{\vec{\alpha}} Y_{\vec{\alpha}}^{(i)}$$

whose components take the form

$$\widehat{C}_{\lambda_1, \lambda_2, \vec{\alpha}}^{(i)} = \{F_i = 0\} \cap H_{i, \lambda_1} \cap H_{i, \lambda_2} \cap Y_{\vec{\alpha}}^{(i)}.$$

These subvarieties meet along varieties

$$\widehat{P}_{\mu_1, \mu_2, \mu_3, \vec{\alpha}}^{(i)} = \{F_i = 0\} \cap H_{i, \mu_1} \cap H_{i, \mu_2} \cap H_{i, \mu_3} \cap Y_{\vec{\alpha}}^{(i)},$$

but they also meet along varieties

$$\widehat{Q}_{\mu_1, \mu_2, \nu_1, \nu_2, \vec{\alpha}}^{(i, j)} = \{F_i = 0\} \cap H_{i, \mu_1} \cap H_{i, \mu_2} \cap H_{j, \nu_1} \cap H_{j, \nu_2} \cap Z_{\vec{\alpha}}^{(i, j)},$$

where

$$Z_{\vec{\alpha}}^{(i, j)} = \bigcap_{\substack{k=1 \\ j \neq i, j}}^r H_{k, \alpha_k}$$

is a toric subvariety of X of codimension $r-2$.

The reason for the extra varieties \widehat{Q} is simple: if we intersect $\widehat{C}_{\lambda_1, \lambda_2, \vec{\alpha}}^{(i)}$ with a toric divisor H_a , then we get something of the form $\widehat{P}_{\lambda_1, \lambda_2, a, \vec{\alpha}}^{(i)}$ if a belongs to the i^{th} part of the partition, but if a belongs to the j^{th} part with $j \neq i$, then we get something of the form $\widehat{Q}_{\lambda_1, \lambda_2, \alpha_j, a, \vec{\alpha}}^{(i, j)}$.

Along intersections of type \widehat{P} , the components of $\pi(\widehat{C})$ are meeting three at a time (as is the case for the original singular locus C); this is illustrated in Figure 2. On the other hand,

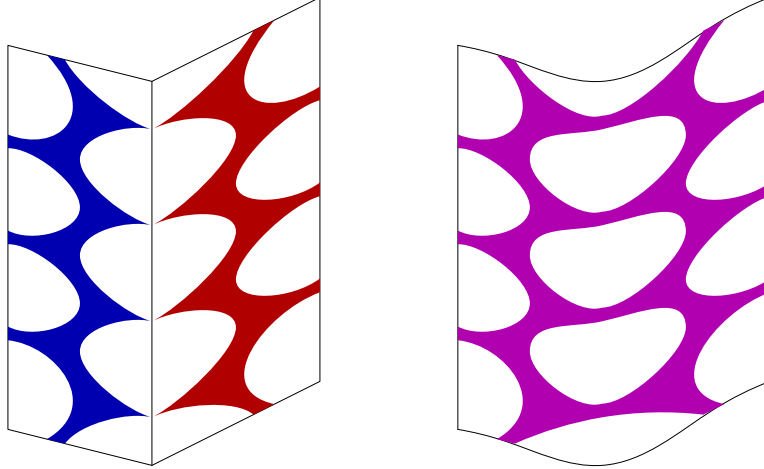


Figure 3: Components of $\pi(\widehat{C}^{(i)})$ meeting two-at-a-time (left), and the deformation to a single component of $\pi(C^{(i)})$ (right).

along intersections of type \widehat{Q} , the components of $\pi(\widehat{C})$ are only meeting two at a time, as illustrated in the left side of Figure 3. Passing back to the original C , components of $\pi(\widehat{C})$ will merge along their two-at-a-time intersections, as illustrated on the right side of Figure 3. The corresponding merger of combinatorial discriminants is illustrated in Figure 4.

Each component $\widehat{C}_{\lambda_1, \lambda_2, \vec{\alpha}}^{(i)}$ is a hypersurface in a toric variety $H_{i, \lambda_1} \cap H_{i, \lambda_2} \cap Y_{\vec{\alpha}}^{(i)}$ of dimension $n - 1$. The moment map for that toric variety maps $\widehat{C}_{\lambda_1, \lambda_2, \vec{\alpha}}^{(i)}$ to an open set $\pi(\widehat{C}_{\lambda_1, \lambda_2, \vec{\alpha}}^{(i)})$ in an $(n-1)$ -dimensional polytope. We expect that the image $\pi(C_{\lambda_1, \lambda_2}^{(i)})$ will degenerate to $\pi(\widehat{C}_{\lambda_1, \lambda_2}^{(i)})$, which is a union of various open subsets of $(n-1)$ -dimensional polytopes, all contained within an n -dimensional space (the moduli space of the T^n 's). We formalize this as follows.

Main Conjecture, continued. *The image of each component of $C^{(i)}$ under π is a deformation of a union of components of $\pi(\widehat{C}^{(i)})$, each of which is an open subset of an $(n-1)$ -dimensional polytope in B , with these components meeting two-at-a-time. The deformation smooths out the intersection points, and is contained in an $(n-1)$ -dimensional submanifold which is a deformation of the union of the corresponding polytopes.*

Upon choosing appropriate triangulation data of the dual polytope, the image of the component of $C^{(i)}$ under π retracts to a codimension one subset of the $(n-1)$ -dimensional submanifold (a part of the combinatorial discriminant of π). This piece of the combinatorial discriminant is a deformation of the union of corresponding degenerate combinatorial discriminant pieces, each of which is the retraction of a component of $\pi(\widehat{C}^{(i)})$ (within the corresponding $(n-1)$ -dimensional polytope).

The degenerate combinatorial discriminant, as a codimension one subset of the union of the polytopes associated to components of \widehat{C} , coincides with the discriminant in the Haase–Zharkov construction [23].

As stated in this part of the Main Conjecture, if we begin with $\pi(\widehat{C}_{\lambda_1, \lambda_2}^{(i)})$, it is a collection

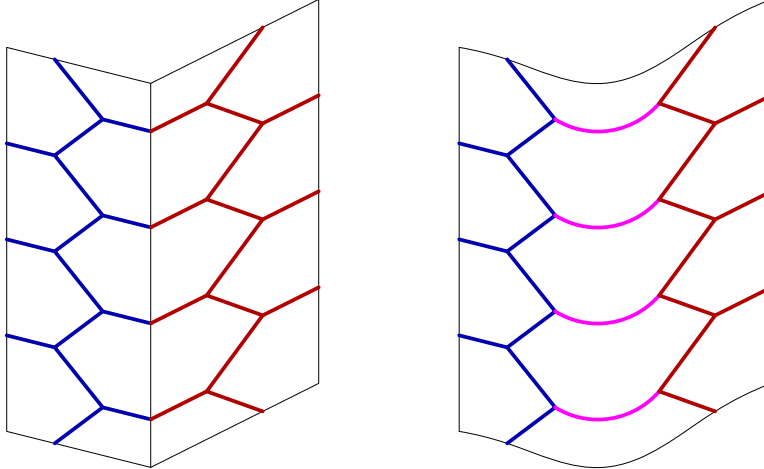


Figure 4: Pieces of $\widehat{D}^{(i)}$ meeting two-at-a-time (left), and the discriminant underlying the smoothing of a pair of components of $\widehat{C}^{(i)}$ to a single component of $C^{(i)}$ (right).

of amoebas in polytopes meeting two-at-a-time. As the union of a pair of ambient polytopes smooths out, their amoebas will join smoothly, as illustrated in Figure 3. At the same time, the corresponding varieties in Z (which map to those two components, and whose intersection is a double point in complex codimension one) smooth to an irreducible variety.

One interesting observation is that the ambient toric varieties of $\widehat{Q}_{\mu_1, \mu_2, \nu_1, \nu_2, \bar{\alpha}}^{(i, j)}$ and $\widehat{Q}_{\nu_1, \nu_2, \mu_1, \mu_2, \bar{\alpha}}^{(j, i)}$ are the same; in the first case, one also imposes $F_i = 0$ while in the second case one imposes $F_j = 0$. The varieties themselves will only meet in codimension 4 of Z , so when $n = 3$ these \widehat{Q} sets are disjoint sets of points. The fact that they live in a common space leads to interesting possibilities for linking and knotting of the combinatorial discriminant, as we shall point out explicitly in the conclusions.

4 The combinatorial discriminant

Haase-Zharkov [23] and Gross [15] produce a combinatorial structure exhibiting some of the expected features of an SYZ fibration. From the combinatorial data determining a mirror pair of complete intersection Calabi–Yau n -folds with trivial canonical class in toric varieties, these authors construct a polytopal complex Σ with the topology of S^n , and two dual affine structures defined on $\Sigma \setminus D$, where the combinatorial discriminant $D \subset \Sigma$ has real codimension 2 (and is a trivalent graph when $n = 3$). These structures were studied in the hypersurface case in [34]. Here we review the construction for a complete intersection, and show by explicit calculation in an example how the combinatorial discriminant D is related to $\pi(C)$. The complete intersection case introduces some additional subtleties into the comparison.

Our example is the intersection $\mathbb{P}^5[4, 2]$ of two hypersurfaces of the indicated degrees in \mathbb{P}^5 . The Batyrev–Borisov construction for this begins with the polytope associated to the

ambient space. This can be written in the lattice $N = \mathbb{Z}^5$ with basis $\{e_i\}_{i=1}^5$ as

$$\nabla^\vee = \text{Conv}(0, e_0, e_1, e_2, e_3, e_4, e_5) \quad (4.1)$$

where $e_0 = -\sum_{i=1}^5 e_i$. Our nef partition is $E^{(1)} = \{e_0, e_1, e_2, e_3\}$, $E^{(2)} = \{e_4, e_5\}$, so that

$$\nabla^\vee = \text{Conv}(\Delta^{(1)}, \Delta^{(2)}) \quad (4.2)$$

with

$$\Delta^{(1)} = \text{Conv}(0, e_0, e_1, e_2, e_3) \quad \Delta^{(2)} = \text{Conv}(0, e_4, e_5) . \quad (4.3)$$

In this case, no triangulation of ∇^\vee is necessary.

The dual polytope ∇ is a reflexive polytope in the dual lattice M . This partition of ∇^\vee induces a decomposition of ∇ as a Minkowski sum

$$\nabla = \nabla^{(1)} + \dots + \nabla^{(r)} . \quad (4.4)$$

This combinatorial construction is perhaps most intuitively understood by considering ∇ as the Newton polytope for a Calabi–Yau hypersurface in X . Explicitly, following the sign notation of [23], we associate to a point m in the dual lattice the monomial $M_m = \prod_a x_a^{1-\langle m, e_a \rangle}$ and thus lattice points in ∇ are associated to monomials with the same degree as $\prod_a x_a$. $\nabla^{(i)}$ then contains those points in ∇ associated to polynomials containing a factor of $\prod_{a \notin E_i} x_a$ and is thus the Newton polytope for sections of the line bundle \mathcal{L}_i . We have $\langle \nabla^{(i)}, \Delta^{(j)} \rangle \leq \delta^{ij}$.

In our example we find

$$\begin{aligned} \nabla = \text{Conv}\{ & 0, [1, 1, 1, 1, 1], [-5, 1, 1, 1, 1], [1, -5, 1, 1, 1], \\ & [1, 1, -5, 1, 1], [1, 1, 1, -5, 1], [1, 1, 1, 1, -5] \} , \end{aligned} \quad (4.5)$$

and the decomposition is $\nabla = \nabla^{(1)} + \nabla^{(2)}$ with

$$\begin{aligned} \nabla^{(1)} = \text{Conv}\{ & 0, [1, 1, 1, 0, 0], [-3, 1, 1, 0, 0], [1, -3, 1, 0, 0], \\ & [1, 1, -3, 0, 0], [1, 1, 1, -4, 0], [1, 1, 1, 0, -4] \} \\ \nabla^{(2)} = \text{Conv}\{ & 0, [0, 0, 0, 1, 1], [-2, 0, 0, 1, 1], [0, -2, 0, 1, 1], \\ & [0, 0, 0, -2, 1, 1], [0, 0, 0, -1, 1], [0, 0, 0, 1, -1] \} \end{aligned} \quad (4.6)$$

Our example enjoys a large symmetry, and this is manifest in the decomposition above. Upon inspection one sees that $\nabla^{(1)}$ is obtained from $\nabla^{(2)}$ by translation (by $[1, 1, 1, -1, -1]$) and doubling. This reflects the fact that we are in $\mathbb{C}\mathbb{P}^n$. We label the vertices of $\nabla^{(i)}$ as $v_a^{(i)}$, $a = 0, \dots, 5$, reflecting this symmetry.

Mirror symmetry in this context is a combinatorial duality [4, 2, 3]. A triangulation of the reflexive polytope

$$\Delta^\vee = \text{Conv}(\nabla^{(1)}, \dots, \nabla^{(r)}) \quad (4.7)$$

determines a dual toric variety, nef partition, and a mirror family of complete intersection Calabi–Yau spaces, and

$$\Delta = \Delta^{(1)} + \dots + \Delta^{(r)} . \quad (4.8)$$

In our example, setting $\Delta^\vee = \text{Conv}(\nabla^{(1)}, \nabla^{(2)})$ we find

$$\Delta = \Delta^{(1)} + \Delta^{(2)} = \text{Conv}\{0, e_a, e_I + e_\alpha\} \quad I \in \{0 \dots 3\}; \quad \alpha \in \{4, 5\} . \quad (4.9)$$

We are interested in studying Z deep inside its Kähler cone – determined by a triangulation of ∇^\vee – and near a complex structure limit point with maximal unipotent monodromy. This corresponds via the monomial-divisor mirror map to a point deep in the Kähler cone of the mirror – determined by a triangulation of Δ^\vee . We thus consider both polytopes to be triangulated.

The construction of [23] produces a polytopal complex Σ in $\Delta \times \nabla$ with the topology of S^3 . Σ is a subdivision of $|\Sigma| = \{(n, m) \in \Delta \times \nabla : \langle n, m \rangle = r\}$ determined by the triangulations of the respective polytopes. We can see some of the structure before triangulating. For a proper face $t \subset \Delta^\vee$ we define $t^{(i)} = t \cap \nabla^{(i)}$. A face will be called *transversal* if none of these are empty. Minimal transversal faces are $r - 1$ simplices with one vertex in each $\nabla^{(i)}$. For a transversal t , $t_\nabla = t^{(1)} + \dots + t^{(r)} \subset \nabla$ is a proper face of ∇ [15]. For a minimal face this is a vertex of ∇ . The dual face to this $s \in \nabla^\vee$ is transversal, i.e. $s^{(i)} = s \cap \Delta^{(i)}$ are all non-empty, and $s_\Delta = s^{(1)} + \dots + s^{(r)}$ is the face of Δ dual to t . Faces $s \subset \Delta^\vee$ and $t \subset \nabla^\vee$ so related are *adjoint* and we have $\dim t_\nabla + \dim s_\Delta = n$. Clearly here $\langle s_\Delta, t_\nabla \rangle = r$ and $|\Sigma|$ is the collection $s_\Delta \times t_\nabla$ for adjoint (s, t) .

In our example, a face s of the simplex ∇^\vee (of any dimension) is transversal if it contains one vertex from each of the $\Delta^{(i)}$. For example, there are 8 irreducible transversal faces $s^{I\alpha} = \text{Conv}\{e_I, e_\alpha\}$, and these produce eight of the vertices of Δ : $s_\Delta^{I\alpha} = e_I + e_\alpha$. With a hopefully obvious notation the transversal faces of ∇^\vee and the faces of Δ that they produce are

$$\begin{aligned} s_\Delta^{IJ\alpha} &= \text{Conv}\{s_\Delta^{I\alpha}, s_\Delta^{J\alpha}\} \\ s_\Delta^{I45} &= \text{Conv}\{s_\Delta^{I4}, s_\Delta^{I5}\} \\ s_\Delta^{IJK\alpha} &= \text{Conv}\{s_\Delta^{IJ\alpha}, s_\Delta^{IK\alpha}, s_\Delta^{JK\alpha}\} \\ s_\Delta^{IJ45} &= \text{Conv}\{s_\Delta^{I4}, s_\Delta^{I5}, s_\Delta^{J4}, s_\Delta^{J5}\} \\ s_\Delta^{0123\alpha} &= \text{Conv}\{s_\Delta^{0\alpha}, s_\Delta^{1\alpha}, s_\Delta^{2\alpha}, s_\Delta^{3\alpha}\} . \end{aligned} \quad (4.10)$$

Note that Δ is not a simplex. The two-dimensional faces we find are either triangles ($\dim s^{(1)} = 2$, $\dim s^{(2)} = 0$) or quadrilaterals ($\dim s^{(1)} = \dim s^{(2)} = 1$).

The six irreducible transversal faces of Δ^\vee are $t^{aa} = \text{Conv}\{v_a^{(1)}, v_a^{(2)}\}$, and they lead to the six vertices of ∇ $t_\nabla^a = v_a^{(1)} + v_a^{(2)}$. The faces of dimension one and two are

$$\begin{aligned} t_\nabla^{IJ} &= \text{Conv}\{t_\nabla^I, t_\nabla^J\} \\ t_\nabla^{I\alpha} &= \text{Conv}\{t_\nabla^I, t_\nabla^\alpha\} \\ t_\nabla^{IJK} &= \text{Conv}\{t_\nabla^I, t_\nabla^J, t_\nabla^K\} \\ t_\nabla^{IJ\alpha} &= \text{Conv}\{t_\nabla^I, t_\nabla^J, t_\nabla^\alpha\} \\ t_\nabla^{IJK\alpha} &= \text{Conv}\{t_\nabla^I, t_\nabla^J, t_\nabla^K, t_\nabla^\alpha\} \end{aligned} \quad (4.11)$$

Sixteen of the twenty triangular two-faces of ∇ are transverse.

The large symmetry of our example makes the duality straightforward: $s_{\Delta}^{\mathcal{I}}$ and $t_{\nabla}^{\mathcal{J}}$ are adjoint faces precisely when $\{0, \dots, 5\} = \mathcal{I} \amalg \mathcal{J}$. More generally, if $s \subset s'$ is a transversal face of s' (implying s' is transversal) and if t is adjoint to s then the adjoint t' to s' is a face of t .

The combinatorial structure is now manifest. The four faces t_{∇}^{IJK} , each adjoint to an edge s_{Δ}^{L45} , form a tetrahedron. The twelve remaining faces $t_{\nabla}^{IJ\alpha}$, adjoint to edges $s_{\Delta}^{KL\beta}$, fall into two groups of six (by α). Along each of the six edges t_{∇}^{IJ} , two of faces of the first type meet two of the second type, one from each family. In accordance with the expected duality, these edges are adjoint to the quadrilateral faces $s_{\Delta}^{KL\alpha\beta}$. Each edge of s is adjoint to one of the intersecting faces. Along the remaining eight edges $t_{\nabla}^{I\alpha}$ the members of each family meet three at a time; these edges are adjoint to the triangular faces s_{Δ}^{JKL} .

A triangulation of ∇^{\vee} and Δ^{\vee} determines, as mentioned above, a suitable limiting point. This induces subdivisions S, T of the boundaries $\partial\nabla^{\vee}$ and $\partial\Delta^{\vee}$ respectively. This in turn induces a subdivision of Σ into cells of the form $(\sigma_{\Delta}, \tau_{\nabla})$ where $\sigma \subset s$ and $\tau \subset t$ are contained in pairs of adjoint faces. The construction of [23, 15] produces a trivalent graph in Σ representing the discriminant of the fibration in the large radius and large complex structure limit.

To construct the discriminant we take the barycentric subdivision associated to Σ . An adjoint pair (σ, τ) is *smooth* if $\dim \sigma^{(i)} \cdot \dim \tau^{(i)} = 0, \forall i$. Vertices of the discriminant are associated to *non-smooth* adjoint pairs. Clearly, if σ or τ is a minimal transversal face the pair is smooth. Non-smooth cells will thus be associated to adjoint pairs for which $\dim \sigma_{\Delta}$ and $\dim \tau_{\nabla}$ are both positive. As a result, both are contained within faces of Δ , resp. ∇ , of dimension at most $n - 1$.

For the purpose of constructing the discriminant, we can thus limit ourselves to the triangulation of these faces. A transversal r -simplex s in the boundary of ∇^{\vee} producing an edge of Δ will have two vertices $e_{i,\lambda_1}, e_{i,\lambda_2}$ lying in one component $\Delta^{(i)}$ and one vertex e_{j,ν_j} in each of the other components. In X this corresponds to the codimension- $r + 1$ toric subvariety $x_{i,\lambda_1} = x_{i,\lambda_2} = x_{j,\nu_j} = 0$. In the terminology of section 2 this is the toric subvariety $H_{i,\lambda_1} \cap H_{i,\lambda_2} \cup Y_{\bar{\alpha}}^{(i)}$ with $\alpha_j = \nu_j \forall j \neq i$.

The dual face t of Δ^{\vee} will be adjoint to s and will produce an $n - 1$ dimensional face of ∇ . Faces of t will be adjoint faces containing s as a face, so all non-smooth cells will be contained in the triangulation of these t . The vertices of D will correspond to the non-smooth cells in the triangulation.

The toric subvariety $H_{i,\lambda_1} \cap H_{i,\lambda_2} \cup Y_{\bar{\alpha}}^{(i)}$ maps to the associated face of ∇^{\vee} under the moment map $\mu : X \rightarrow N_{\mathbb{R}}$, and the combinatorial version of the conjecture is that the projection of the component $C_{\lambda_1, \lambda_2, \bar{\alpha}}^{(i)}$ retracts to the graph so constructed. We will not prove this in general.

In our example, the fact that ∇^{\vee} requires no subdivision makes things simple. The transversal two-faces producing edges of Δ are dual to the three-faces of Δ^{\vee} producing the two types of two-dimensional faces of ∇ described above. Our job is to triangulate these. The existence of a subdivision of the polytope consistent with our choices is supported by the consistency of our results, although we have not proved it.

Consider first the one-dimensional cell τ_{∇}^{01} . The two-dimensional transverse face producing this is the trapezoid with vertices $v_0^{(1)}, v_1^{(1)}, v_0^{(2)}, v_1^{(2)}$. Subdividing this as in Figure 5 we

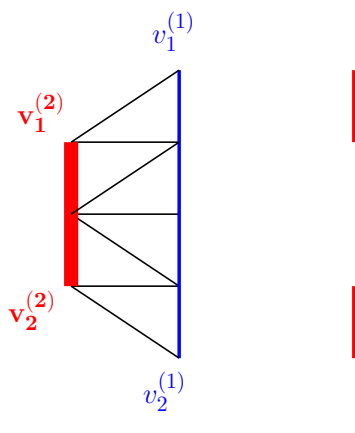


Figure 5: Triangulation of a trapezium leading to the subdivision of an interval.

find six cells and the resulting division of $\tau^{(01)}$ is indicated. The six cells into which the segment is subdivided are colored to indicate that four of them have $\dim \tau^{(1)} = 1, \dim \tau^{(2)} = 0$ while two have $\dim \tau^{(1)} = 0, \dim \tau^{(2)} = 1$. We assume that we can make this subdivision for each of the 14 transversal edges.

We now need to consider the two-dimensional cells of either type. These will all be equilateral triangles with sides of length six as we have seen above. Each is obtained from a three-dimensional face of Δ^\vee intersecting $\Delta^{(i)}$ in two parallel triangles of side lengths four and two, as in Figure 6. The region between those triangles consists of triangular prisms which must be further subdivided. Our subdivision includes three kinds of simplices. The first type, indicated in boldface (red) type in the figure, meets the larger triangle at a vertex and the smaller in a face and so has dimensions $(\dim \tau^{(1)}, \dim \tau^{(2)}) = (0, 2)$. The second type, indicated with ordinary (blue) type in the figure, inverts this and has dimensions $(2, 0)$. A third type, indicated by the dashed (green) sides, meets each triangle along a side so has dimensions $(1, 1)$. Figure 7 shows how these three types arise in subdividing a prism. As with the interval in Figure 5, we obtain an induced subdivision of the two-dimensional face by taking Minkowski sums. The sum of a triangle and a point leads to triangles of the two types shown in Figure 8. The sum of two intervals is a parallelogram, leading to the (green) cells that pair up two dashed edges. The figure illustrates that this is compatible with our subdivision of the edges, in that the two segments of each side that are associated to $\nabla^{(2)}$ are in the positions in which we need them.

With our subdivision in hand we can now find the non-smooth pairs whose centers will form the vertices of our graph for the discriminant. Non-smooth cells with $(\dim \sigma_\Delta, \dim \tau_\nabla) = (1, 2)$ occur on the large triangles just discussed. As mentioned above, there are two types of these faces. Faces of the first type, τ_∇^{LJK} , are paired with one-dimensional cells such as σ_Δ^{L45} . These have dimensions $(0, 1)$ so non-smooth pairs will result when the subdivided τ has nonzero dimensional intersection with $\nabla^{(2)}$, i.e., for the bold (red) and dashed (green) cells as indicated in Figure 9.

These faces correspond, as discussed above, to the four toric subvarieties $H_{1,L} \cap H_{2,4} \cap H_{2,5}$. In the limit in which $F_1 = x_0 x_1 x_2 x_3$ the (single) component $C_{45}^{(2)}$ restricts to the union of

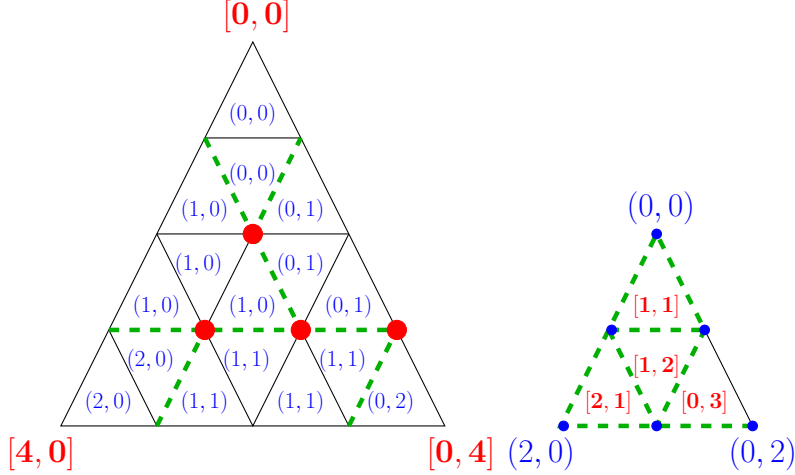


Figure 6: How to match the triangles of different sizes. The large (red) vertices on the left are paired with correspondingly-labeled faces on the right, and the small (blue) vertices on the right are paired with faces on the left. The dashed (green) edges pair up between the triangles, to span simplices between them. (For example, the edge between $[2, 1]$ and $[1, 2]$ pairs with the edge between $(1, 0)$ and $(1, 1)$.)

these as a plane conic in each \mathbb{P}^2 . Note that here $\widehat{P}^{(2)}$ is empty.

The twelve faces of the other type $\tau_{\nabla}^{IJ\alpha}$, are paired with one-dimensional cells $\sigma_{\Delta}^{KL\beta}$ with dimensions $(1, 0)$. Here non-smooth pairs arise from cells with nonzero dimensional intersection with $\nabla^{(1)}$, i.e., the non-bold (blue) and dashed (green) cells as indicated in Figure 10.

These correspond to the twelve toric subvarieties $H_{1,K} \cap H_{1,L} \cap H_{2,\beta}$. In the limit in which $F_2 = x_4 x_5$ the components of $C^{(1)}$ restrict to the union of these as plane quartics in each \mathbb{P}^2 .

Note that each of the quadrilateral (green) cells adjoins two non-smooth cells (along a non-smooth edge) and two smooth cells (along a smooth edge) so that these cells lead to bivalent vertices. The adjacent smooth cells show that the monodromy about the two edges meeting at such a vertex is the same.

We can now compute the Euler character of Z , which is predicted to be the difference of the number of positive and negative vertices of D . Each of the four faces τ^{IJK} has four negative vertices (note that the bivalent vertices can be smoothed and do not contribute to the Euler character), while each of the twelve faces $\tau^{IJ\alpha}$ has 16 negative vertices, for a total of 208 negative vertices.

The positive vertices are associated to non-smooth cells with $(\dim \sigma_{\Delta}, \dim \tau_{\nabla}) = (2, 1)$. These arise, as discussed above, along the edges of the large faces. (non-smooth internal edges connect two non-smooth cells so the associated vertex is a simple double point and does not contribute to our Euler characteristic). As mentioned above, there are two types of edges. At an edge τ_{∇}^{IJ} two faces of each type meet. Since the associated σ_{Δ}^{KL45} has dimensions $(1, 1)$ all cells are non-smooth. The σ_{Δ} cells are quadrilaterals and as was the case above, each connects two non-smooth cells (belonging to faces of identical type) along a non-smooth edge and two smooth cells (belonging to the faces of the other type) along a smooth edge.

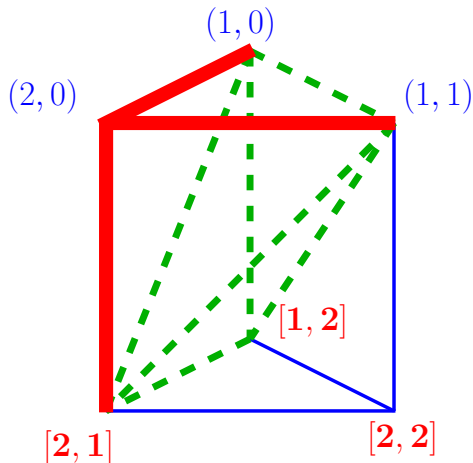


Figure 7: Triangulating a prism. The upper triangle is a sub-triangle of the right side of Figure 6, while the lower triangle is a sub-triangle of the left side of Figure 6.

Thus the six quadrilaterals along each of these large edges are all bivalent vertices (oriented in two different ways) connecting faces of the same type. All of this contributes nothing to the Euler characteristic.

These edges are associated to the toric subvarieties $H_{1,K} \cap H_{1,L} \cap H_{2,4} \cap H_{2,5}$. As discussed above, we see that these contain both the intersections $\widehat{Q}_{KL45}^{(1,2)}$ and $\widehat{Q}_{45KL}^{(2,1)}$ (for $r = 2$ the $Z^{(1,2)}$ are just X). These are generically disjoint two-at-a-time intersections of pairs of components of $C^{(1)}$ and $C^{(2)}$.

The other type of edge $\tau_{\nabla}^{I\alpha}$, along which three faces of the second type meet, is paired with a cell $\sigma^{JKL\beta}$ of dimensions $(1, 0)$. Segments of the edge with nonzero dimensional intersection with $\nabla^{(1)}$ (the four blue segments) are non-smooth. These are precisely the edges bounding non-smooth cells, and so each such edge contributes four trivalent vertices. There are eight such edges and hence 32 positive vertices.

These are associated to $H_{1,J} \cap H_{1,K} \cap H_{1,L} \cap H_{2,\beta}$ and contain the intersections $\widehat{P}_{JKL\beta}^{(1)}$.

Adding up the contributions to the Euler characteristic we find $32 - 208 = -176$ as expected.

5 Concluding Remarks

Strominger, Yau, and Zaslow applied physics arguments to a string-theoretic version of mirror symmetry, obtaining a remarkable prediction about mathematics. An understanding of the structure of the fibration whose existence they predicted could provide insights into both Calabi–Yau geometry and mirror symmetry. The geometric conjectures of [34] are geometrically natural but some of the strongest evidence for them was their compatibility with the combinatorial constructions of [21, 22] (which provided a general formulation of the original constructions given by Gross and by Ruan). The extension of these combinatorial constructions to complete intersections is quite nontrivial. The fact that the conjecture extends naturally in a way that appears compatible with this more elaborate construction

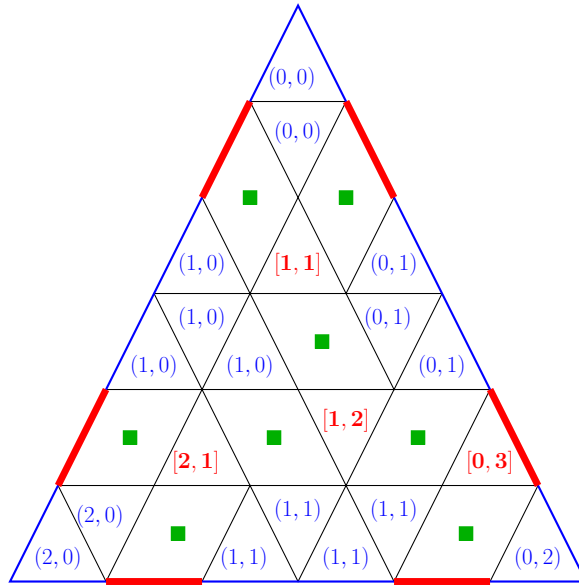


Figure 8: The corresponding large triangle, with both types of faces, labeled in bold (red) type and non-bold (blue) type. The square (green) vertices mark faces which are the Minkowski sums of a pair of dashed (green) edges from the previous figures.

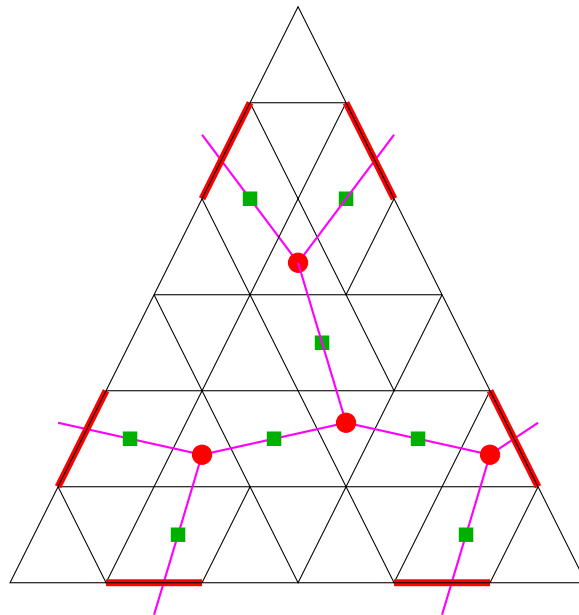


Figure 9: The triangulation with large (red) and square (green) vertices.

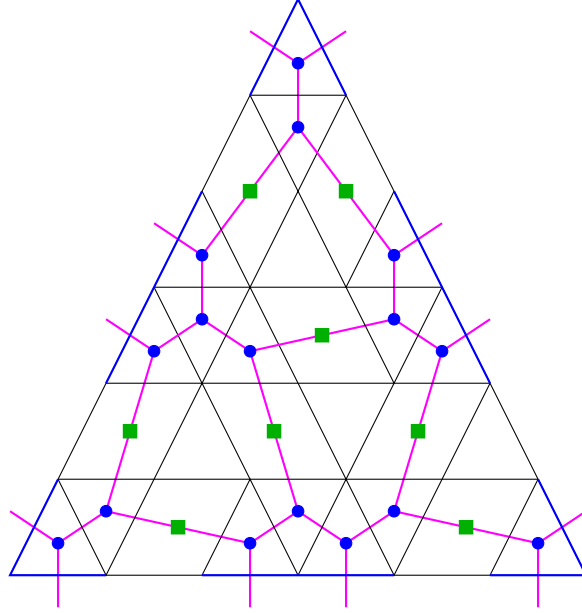


Figure 10: The triangulation with small (blue) and square (green) vertices.

is encouraging.

One new feature of the complete intersection construction is that in general the components of the combinatorial discriminant, graphs in S^3 for $n = 3$, will be linked and (possibly) knotted. We have not attempted to compute this in general.

Note that in this paper we have not proved the compatibility of our conjectured construction with the complete intersection combinatorics but have simply checked it in an example. It should be possible to show that for any choice of triangulation data that fully specifies the discriminant in the combinatorial construction of [23], the images under π of the components of \widehat{C} do indeed retract to pieces of the discriminant; we have not attempted this. In particular, the detailed structure of D depends on a choice of triangulation, or equivalently a choice of a limiting point of maximally unipotent monodromy in moduli space. Different choices of triangulation of ∇^\vee are related by flop transitions, and understanding the way the fibration changes in these would be useful.

Mirror symmetry was an essential ingredient in the original argument for the existence of a fibration and one of the most intriguing predictions is that the fibrations of two members of a mirror pair are related by a simple duality. One attractive feature of the combinatorial construction is that it implements this duality very naturally. The combinatorial construction for the mirror of Z is obtained by exchanging the roles of Δ and ∇ . The construction of Σ is clearly invariant under this. Moreover the construction leads naturally to two dual integral affine structures sharing the same discriminant.

The way in which the conjecture is compatible with this symmetry is obscured by the simple nature of our example, so it perhaps bears mention. In our example, ∇^\vee was a simplex and the combinatorial structure was essentially determined by the triangulation of Δ^\vee : all the cells in a triangulation of a face of Δ^\vee were paired with the same face of ∇^\vee . In a more general

example, the face of ∇^V would also be triangulated. For example, in the combinatorial construction for the mirror of our example – a codimension two complete intersection in a toric variety determined by a triangulation of Δ^V – if we choose the triangulation used here, the red triangles in faces would be associated to the ambient space of $\widehat{P}^{(2)}$, the blue triangles to the ambient space of $\widehat{P}^{(1)}$, and the quadrilateral cells to the common ambient space of $\widehat{Q}^{(1,2)}$ and $\widehat{Q}^{(2,1)}$.

Acknowledgements: We are grateful to P.S. Aspinwall, M. Bertolini, R. Castaño-Bernard, C. Haase, and X. de la Ossa for helpful conversations, and to D.-E. Diaconescu for collaboration in the early stages of this work. MRP thanks the Mathematics department at UCSB for gracious hospitality during essential phases of this work. DRM is supported by NSF grant PHY-1307513, and MRP is supported by NSF grant PHY-1217109. Any opinions, findings, and conclusions or recommendations expressed in this material are those of the authors and do not necessarily reflect the views of the National Science Foundation.

References

- [1] P. S. Aspinwall, C. A. Lütken, and G. G. Ross, *Construction and couplings of mirror manifolds*, Phys. Lett. B **241** (1990) 373–380.
- [2] V. V. Batyrev and L. A. Borisov, *Dual cones and mirror symmetry for generalized Calabi–Yau manifolds*, Mirror symmetry, II, AMS/IP Stud. Adv. Math., vol. 1, Amer. Math. Soc., Providence, RI, 1997, pp. 71–86, [arXiv:alg-geom/9402002](#).
- [3] ———, *On Calabi–Yau complete intersections in toric varieties*, Higher-dimensional complex varieties (Trento, 1994), de Gruyter, Berlin, 1996, pp. 39–65, [arXiv:alg-geom/9412017](#).
- [4] L. A. Borisov, *Towards the mirror symmetry for Calabi–Yau complete intersections in Gorenstein toric Fano varieties*, [arXiv:alg-geom/9310001](#).
- [5] E. Calabi, *On Kähler manifolds with vanishing canonical class*, Algebraic Geometry and Topology, A Symposium in Honor of S. Lefschetz (R. H. Fox et al., eds.), Princeton University Press, Princeton, 1957, pp. 78–89.
- [6] P. Candelas, M. Lynker, and R. Schimmrigk, *Calabi–Yau manifolds in weighted \mathbb{P}_4* , Nuclear Phys. B **341** (1990) 383–402.
- [7] D. A. Cox, *The homogeneous coordinate ring of a toric variety*, J. Algebraic Geom. **4** (1995) 17–50, [arXiv:alg-geom/9210008](#).
- [8] P. Deligne, *Local behavior of Hodge structures at infinity*, Mirror symmetry, II, AMS/IP Stud. Adv. Math., vol. 1, Amer. Math. Soc., 1997, pp. 683–699.
- [9] H. Federer, *Geometric measure theory*, Die Grundlehren der mathematischen Wissenschaften, Band 153, Springer-Verlag New York Inc., New York, 1969.

- [10] W. Fulton, *Introduction to toric varieties*, Annals of Math. Studies, vol. 131, Princeton University Press, Princeton, 1993.
- [11] B. R. Greene and M. R. Plesser, *Duality in Calabi–Yau moduli space*, Nucl. Phys. B **338** (1990) 15–37.
- [12] M. Gross, *Special Lagrangian fibrations. I. Topology*, Integrable systems and algebraic geometry (Kobe/Kyoto, 1997), World Sci. Publishing, River Edge, NJ, 1998, pp. 156–193, [arXiv:alg-geom/9710006](#).
- [13] ———, *Special Lagrangian fibrations. II. Geometry. A survey of techniques in the study of special Lagrangian fibrations*, Surveys in differential geometry: differential geometry inspired by string theory, Surv. Differ. Geom., vol. 5, International Press, Cambridge, 1999, pp. 341–403, [arXiv:math.AG/9809072](#).
- [14] ———, *Topological mirror symmetry*, Invent. Math. **144** (2001) 75–137, [arXiv:math.AG/9909015](#).
- [15] ———, *Toric degenerations and Batyrev–Borisov duality*, Math. Ann. **333** (2005) 645–688, [arXiv:math.AG/0406171](#).
- [16] ———, *Mirror symmetry and the Strominger–Yau–Zaslow conjecture*, Current developments in mathematics 2012, Int. Press, Somerville, MA, 2013, pp. 133–191, [arXiv:arXiv:1212.4220](#) [math.AG].
- [17] M. Gross and B. Siebert, *Affine manifolds, log structures, and mirror symmetry*, Turkish J. Math. **27** (2003) 33–60, [arXiv:math.AG/0211094](#).
- [18] ———, *Mirror symmetry via logarithmic degeneration data. I*, J. Differential Geom. **72** (2006) 169–338, [arXiv:math.AG/0309070](#).
- [19] ———, *Mirror symmetry via logarithmic degeneration data, II*, J. Algebraic Geom. **19** (2010) 679–780, [arXiv:0709.2290](#) [math.AG].
- [20] ———, *From real affine geometry to complex geometry*. Ann. of Math. (2) **174** (2011) 1301–1428, [arXiv:math.AG/0703822](#).
- [21] C. Haase and I. Zharkov, *Integral affine structures on spheres and torus fibrations of Calabi–Yau toric hypersurfaces I*, [arXiv:math.AG/0205321](#).
- [22] ———, *Integral affine structures on spheres and torus fibrations of Calabi–Yau toric hypersurfaces II*, [arXiv:math.AG/0301222](#).
- [23] ———, *Integral affine structures on spheres: complete intersections*, Int. Math. Res. Not. (2005) 3153–3167, [arXiv:math.AG/0504181](#).
- [24] R. Harvey and H. B. Lawson, Jr., *Calibrated geometries*, Acta Math. **148** (1982) 47–157.
- [25] N. Hitchin, *The moduli space of special Lagrangian submanifolds*, Annali Scuola Sup. Norm. Pisa Sci. Fis. Mat. **25** (1997) 503–515, [arXiv:dg-ga/9711002](#).

- [26] D. Joyce, *Singularities of special Lagrangian fibrations and the SYZ conjecture*, Comm. Anal. Geom. **11** (2003) 859–907, [arXiv:math.DG/0011179v3](#).
- [27] ———, *U(1)-invariant special Lagrangian 3-folds. I. Nonsingular solutions*, Adv. Math. **192** (2005) 35–71, [arXiv:math.DG/0111324](#).
- [28] ———, *U(1)-invariant special Lagrangian 3-folds. II. Existence of singular solutions*, Adv. Math. **192** (2005) 72–134, [arXiv:math.DG/0111326](#).
- [29] ———, *U(1)-invariant special Lagrangian 3-folds. III. Properties of singular solutions*, Adv. Math. **192** (2005) 135–182, [arXiv:math.DG/0204343](#).
- [30] R. C. McLean, *Deformations of calibrated submanifolds*, Comm. Anal. Geom. **6** (1998) 705–747.
- [31] D. R. Morrison, *Compactifications of moduli spaces inspired by mirror symmetry*, Journées de Géométrie Algébrique d’Orsay (Juillet 1992), Astérisque, vol. 218, Société Mathématique de France, 1993, pp. 243–271, [arXiv:alg-geom/9304007](#).
- [32] ———, *Mirror symmetry and rational curves on quintic threefolds: A guide for mathematicians*, J. Amer. Math. Soc. **6** (1993) 223–247, [arXiv:alg-geom/9202004](#).
- [33] ———, *Geometric aspects of mirror symmetry*, Mathematics Unlimited – 2001 and Beyond (B. Enquist and W. Schmid, eds.), Springer-Verlag, 2001, pp. 899–918, [arXiv:math.AG/0007090](#).
- [34] ———, *On the structure of supersymmetric T^3 -fibrations*, Tropical Geometry and Mirror Symmetry (R. Castaño-Bernard, Y. Soibelman, and I. Zharkov, eds.), Contemp. Math., vol. 527, Amer. Math. Soc., Providence, RI, 2010, pp. 91–112, [arXiv:1002.4921](#) [[math.AG](#)].
- [35] W.-D. Ruan, *Lagrangian torus fibration of quintic hypersurfaces. I. Fermat quintic case*, Winter School on Mirror Symmetry, Vector Bundles and Lagrangian Submanifolds (Cambridge, MA, 1999), AMS/IP Stud. Adv. Math., vol. 23, Amer. Math. Soc., 2001, pp. 297–332, [arXiv:math.DG/9904012](#).
- [36] ———, *Lagrangian torus fibration of quintic Calabi–Yau hypersurfaces. II. Technical results on gradient flow construction*, J. Symplectic Geom. **1** (2002) 435–521, [arXiv:math.SG/0411264](#).
- [37] ———, *Lagrangian torus fibration of quintic Calabi–Yau hypersurfaces. III. Symplectic topological SYZ mirror construction for general quintics*, J. Differential Geom. **63** (2003) 171–229, [arXiv:math.DG/9909126](#).
- [38] ———, *Lagrangian torus fibration and mirror symmetry of Calabi–Yau hypersurface in toric variety*, [arXiv:math.DG/0007028](#).
- [39] ———, *Lagrangian torus fibrations and mirror symmetry of Calabi–Yau manifolds*, Symplectic geometry and mirror symmetry (Seoul, 2000), World Sci. Publishing, 2001, pp. 385–427, [arXiv:math.DG/0104010](#).

- [40] ———, *Newton polygon and string diagram*, *Comm. Anal. Geom.* **15** (2007) 77–119, [arXiv:math.DG/0011012](#).
- [41] ———, *Generalized special Lagrangian torus fibration for Calabi–Yau hypersurfaces in toric varieties. I*, *Commun. Contemp. Math.* **9** (2007) 201–216, [arXiv:math.DG/0303114](#).
- [42] ———, *Generalized special Lagrangian torus fibration for Calabi–Yau hypersurfaces in toric varieties II*, *Mirror Symmetry V* (N. Yui, S.-T. Yau, and J. D. Lewis, eds.), American Mathematical Society and International Press, 2007, [arXiv:math.DG/0303278](#).
- [43] ———, *Generalized special Lagrangian fibration for Calabi–Yau hypersurfaces in toric varieties III: The smooth fibres*, [arXiv:math.DG/0309450](#).
- [44] A. Strominger, S.-T. Yau, and E. Zaslow, *Mirror symmetry is T-duality*, *Nucl. Phys. B* **479** (1996) 243–259, [arXiv:hep-th/9606040](#).
- [45] S.-T. Yau, *Calabi’s conjecture and some new results in algebraic geometry*, *Proc. Nat. Acad. Sci. U.S.A.* **74** (1977) 1798–1799.
- [46] S. T. Yau, *On the Ricci curvature of a compact Kähler manifold and the complex Monge-Ampère equation. I*, *Comm. Pure Appl. Math.* **31** (1978) 339–411.
- [47] I. Zharkov, *Torus fibrations of Calabi–Yau hypersurfaces in toric varieties*, *Duke Math. J.* **101** (2000) 237–257, [arXiv:math.AG/9806091](#).